Zwitterionic Polymers towards the Development of Orientation-Sensitive Bioprobes

Zijun Wang, Fanny Delille, Sophie Bartier, Thomas Pons, Nicolas Lequeux, Bruno Louis, Jongwook Kim, Thierry Gacoin

▶ **To cite this version:**

Zijun Wang, Fanny Delille, Sophie Bartier, Thomas Pons, Nicolas Lequeux, et al.. Zwitterionic Polymers towards the Development of Orientation-Sensitive Bioprobes. Langmuir, 2022, 38 (34), pp.10512-10519. ⟨10.1021/acs.langmuir.2c01286⟩. ⟨inserm-03780613⟩

HAL Id: inserm-03780613

https://inserm.hal.science/inserm-03780613v1

Submitted on 19 Sep 2022

HAL is a multi-disciplinary open access archive for the deposit and dissemination of scientific research documents, whether they are published or not. The documents may come from teaching and research institutions in France or abroad, or from public or private research centers.

L'archive ouverte pluridisciplinaire **HAL**, est destinée au dépôt et à la diffusion de documents scientifiques de niveau recherche, publiés ou non, émanant des établissements d'enseignement et de recherche français ou étrangers, des laboratoires publics ou privés.

HAL Authorization

Zwitterionic Polymers towards the Development of Orientation-Sensitive Bioprobes

Zijun Wang,[a] Fanny Delille,[b] Sophie Bartier,[c] Thomas Pons,[b] Nicolas Lequeux,[b] Bruno Louis,[c] Jongwook Kim[a] and Thierry Gacoin*[a]*

[a.] Laboratoire de Physique de la Matière Condensée, Ecole Polytechnique, CNRS, IP Paris, 91128 Palaiseau, France.

[b.] Laboratoire de Physique et d'Étude des Materiaux, ESPCI Paris, PSL Research University, CNRS, Sorbonne Université, 75005, Paris, France.

[c.] Université Paris Est Créteil, IMRB, INSERM, CNRS, 94010, Créteil, France.

ABSTRACT: Dynamics with an orientational degree of freedom are fundamental in biological events. Probes with polarized luminescence enable a determination of the orientation. Lanthanide-doped nanocrystals can provide more precise analysis than quantum dots due to the non-photoblinking/bleaching nature and the multiple line-shaped emission. However, the intrinsic polarization property of the original nanocrystals often deteriorates in complex physiological environments, because the colloidal stability easily breaks and the probes aggregate in the media with abundant salts and macromolecules. Engineering the surface chemistry of the probes is thus essential to be compatible with biosystems, which has remained a challenging task that should be exclusively addressed for each specific probe. Here, we demonstrate a facile and efficient surface functionalization of lanthanide-doped nanorods by zwitterionic block copolymers. Due to the steric interaction and the intrinsic zwitterionic nature of the polymers, high colloidal stability of the zwitterionic nanorod suspension is achieved over wide ranges of pH and concentration of salts, even giving rise to the lyotropic liquid crystalline behavior of the nanorods in physiological media. The shear-aligned ability is shown to be unaltered by the coated polymers and thus the strongly polarized emission of Eu^{3+} is preserved. Besides, biological experiments reveal good biocompatibility of the zwitterionic nanorods with negligible non-specific binding. This study is a stepping stone for the use of the nanorods as orientation probes in biofluids and validates the strategy of coupling zwitterions to lanthanide-doped nanocrystals for various bio-applications.

KEYWORDS: zwitterion, functionalization, nanorod, lanthanide, polarization, bio-application

INTRODUCTION

Luminescent nanocrystals are attracting extensive attention both in fundamental research and in emerging applications due to their abundant tunability over various parameters, such as particle sizes and crystalline structures of particles.[1,2] Synthetic protocols have been maturely developed for the elaboration of nanocrystals with tuned size and shape.[3,4] When the shape of the particle is anisotropic (e.g. rods or plates), the intrinsic polarization properties can be detected explicitly, linking the anisotropy axis with respect to the spatial orientation of the particle.[5-7] Taking advantage of the polarization properties from anisotropic nanocrystals, one can thus determine the orientation of a specific particle or the strength of the external forces stimulating the orientation of collective particles.[8-11]

This orientation analysis is of special interest in biological fields, as many physiological phenomena involve the conformational changes, dynamics, and fluctuations of macromolecules.[12] As an example, Yanagida et.al revealed the dynamic movements of biological macromolecules using the polarization technique of a binding quantum rod.[8] Recently, our group has developed a technique for monitoring shear stress in microfluidics using the polarized emission of Eu^{3+} doped in the shear-aligned nanorods.[13] The nanorods show promising potential in biological fields, not only as orientation probes but also as imaging labels and sensors. Nevertheless, good colloidal stability is only available under acid conditions (pH=2-3). Targeting the biological applications, the conventional synthetic protocols hardly can produce the nanocrystals that are directly compatible with bio-environments.[11] The presence of the salts and macromolecules, as well as the pH in the physiological environments, can induce the aggregation of nanocrystals. Therefore, subsequent surface engineering is requisite for the nanocrystals to preserve their functionality and adapt to harsh physiological environments.

Various approaches have been applied to ensure the appropriate surface functionalization, such as encapsulation and ligand exchange.[1,14] Polymeric ethylene glycol (PEG) is the most used ligand to achieve biocompatibility, hydrophilicity, and access to further bioconjugation.[15-18] However, the drawbacks of PEG include low tolerance to salts and a dramatic increase in the hydrodynamic diameter of the PEG-coupled nanocrystals.[19-21] Degradation of PEG can also occur in the presence of oxygen and transition metals.[22,23] As an interesting alternative, oligomeric or polymeric zwitterionic ligands have been exploited recently[21,24] By virtue of the positive and negative charges in different functionalized groups under an internal balance, strong anti-fouling properties, and minimization or elimination of non-specific binding can be realized.[25-27] Also, there is a limited increase of hydrodynamic diameter for the functionalized nanocrystals as zwitterionic ligands can provide near monolayer-type coverage on the particle surface.[20] Different combinations of the nature and the structure for the zwitterion moieties can tune the charge density and thus the hydration ability.[27,28] High water solubility of zwitterionic polymers is then realized because of the strongly formed hydration layers via electrostatic interactions, which discriminates zwitterions from PEG with weak hydrogen bonds.[23,29] All these features can benefit the uptake,

biodistribution, and removal of circulating nanoparticles for *in vitro* and *in vivo* experiments.[30]

Until now, the zwitterionic ligands have been widely applied to bio-purposed inorganic nanoparticles, such as quantum dots, gold, and silica.[21,25] Although the quantum dots and the lanthanide-doped nanocrystals exhibit luminescence, the origin of their emission is significantly different because of the distinctive nature of the composition (semiconductor and dielectric). Usually, strong affinity is favored by interactions of S- and N-contained groups (e.g. thiolate or imidazole) to quantum dots,[31,32] while O-contained groups (e.g. phosphonate, silane, or carboxyl) are used to bind to lanthanide-doped materials.[15,18,33] This demonstrates the significance of the rational design of zwitterionic functions and attaching groups to the lanthanide-doped nanocrystals. Moreover, our specific nanorod system should meet an extra demand to preserve the perfect orientability of the nanorods after coupling with functionalized agents if used for the orientation analysis.

In the present work, efficient functionalization is realized by coupling poly(phosphonate-zwitterionic) block copolymers to the bare $LaPO_4$ nanorods and enhanced under microwave heating. The phosphonate block anchors stably to the nanorod surface thanks to multidentate interactions, while the zwitterionic sulfobetaine moieties provide a highly hydrophilic coating. Colloidal stability was investigated for the resulting zwitterion functionalized nanorods in terms of time, electrolyte species and concentration, and pH value. The hydrophilicity and biocompatibility were demonstrated by the observed liquid crystalline behavior and *in vitro* cellular experiments. Besides, strong polarization of Eu^{3+} emission was shown to be preserved on the aligned nanorods, enabling further targeting for the orientation analysis in biofluids.

RESULTS AND DISCUSSION

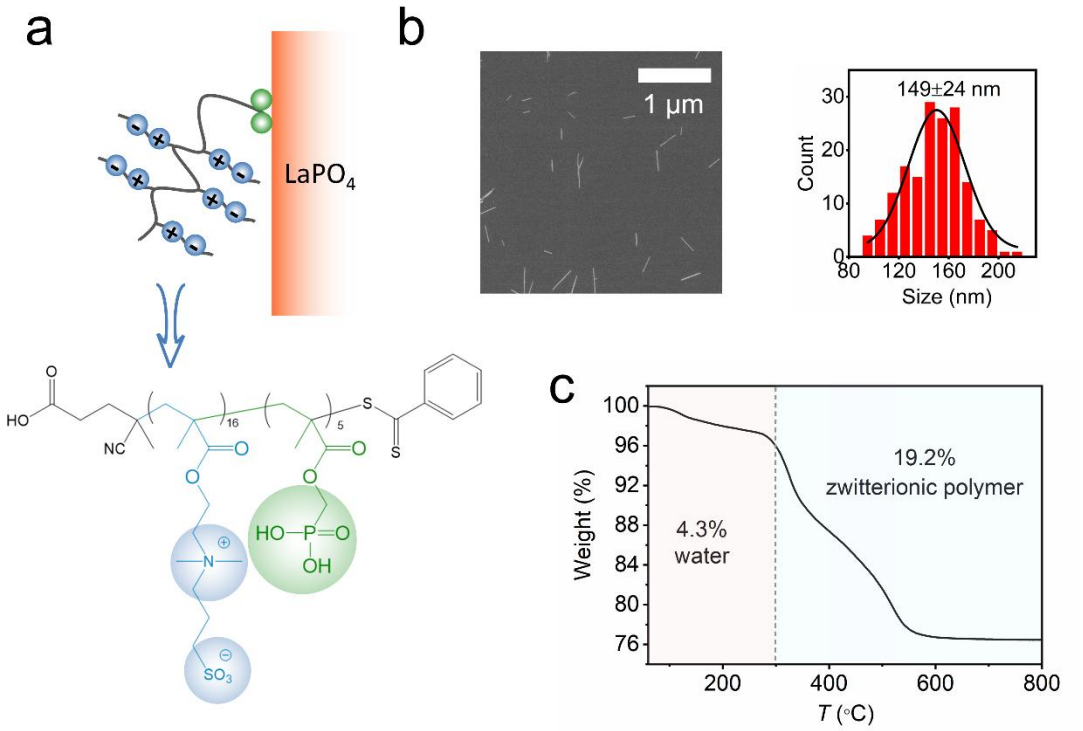

Figure 1. Zwitterionic functionalization of $LaPO_4$:5%Eu^{3+} nanorods. (a) Scheme of functionalization by the p(MAPC1-b-SBMA) zwitterionic polymer on a nanorod with the molecule structure. (b) SEM image of the functionalized nanorods with a histogram of length distribution. (c) Thermogravimetric analysis of the functionalized nanorods heating from room temperature to 800°C at a rate of 10°C/min.

Zwitterionic Functionalization by p(MAPC1-b-SBMA) Polymer The zwitterionic block copolymers (Mn = 5300 g/mol, **Figure 1a**) used for the surface functionalization were synthesized by reversible addition-fragmentation chain transfer polymerization.[34] The two blocks are constructed from (methacryloyloxy)methyl phosphonic acid (MAPC1) and sulfobetaine methacrylate (SBMA) monomers with 4-cyanopentanoic acid dithiobenzoate as the chain transfer agent.[35,36] The final polymer contains on average 5 phosphonic acid groups and 16 sulfobetaine moieties, as determined by nuclear magnetic resonance spectroscopy and gel permeation chromatography. The design of the MAPC1 block is aimed at dense coverage of ligands on the nanocrystal surface and strong anchoring points by the phosphonate groups due to the multidentate effects.[29,31,32,37,38] We found that five phosphonate groups are efficient enough to ensure a stable anchoring of the polymer to the nanorods. The sulfobetaine moiety with its positively charged quaternary ammonium group and negatively charged sulfonate group retains a zwitterionic character independently of pH and endows the polymer with high hydrophilicity. In our previous work, the functionalization and stabilization of nanocrystals by sulfobetaine based copolymers work efficiently in a range of sulfobetaine block length between 3,000 and 20,000 g/mol.[27] **Figure S1** shows the excitation and emission spectra for this p(MAPC1-b-SBMA) zwitterionic polymer dispersed in water.

There is a broad absorption band at 290 nm and a broad emission band at 350 nm. The UV absorption is ascribed to the dithiobenzoate end group of the chain transfer agent, which induces a light pink color of the dried p(MAPC1-b-SBMA) polymer.[39]

The nanocrystals in this study are the monazite $LaPO_4$:5%Eu^{3+} nanorods synthesized in our previous work.[40] The nanorods with bare surfaces are colloidally stabilized only in acidic polar media (pH=1-3) by electrostatic repulsion from the surface charges. To implement the zwitterionic surface functionalization, the original nanorods were mixed with p(MAPC1-b-SBMA) polymer under sonication for 1 h. Subsequently, the pH of the mixture should be tuned to near neutral so that the phosphonic acid in the MAPC1 groups can be deprotonated to efficiently bind to the nanorod surface (La^{3+} and Eu^{3+} ions). Then, the functionalization proceeded by microwave heating at 100°C for 1 h, dramatically improving the colloidal quality, which will be addressed later. The details of the functionalization protocol are provided in the **Supporting Information** (**SI**).

The image of scanning electron microscopy (SEM) in **Figure 1b** demonstrates a good monodispersity of the functionalized nanorods without aggregates. The calculated average length is 150 nm and the corresponding aspect ratio is 18-35. To validate the coupling of p(MAPC1-b-SBMA) polymer, the nanorods after a thorough wash were characterized by Fourier transform infrared (FT-IR, **Figure S2**) spectra and thermogravimetric analysis (TGA, **Figure 1c**). For the bare nanorods, P-O antisymmetric stretching vibrations occur at 1066 and 993 cm^{-1}, and symmetric stretching vibrations appear at 953 cm^{-1}. The bands at 542, 583, and 613 cm^{-1} belong to the O-P-O antisymmetric bending.[41] After the zwitterionic functionalization, new bands appear at 1385, 2876, and 2961 cm^{-1} for -CH_3 vibrations, and 1462, 2839, and 2918 cm^{-1} for -CH_2 vibrations,[42] confirming the successful coupling of the zwitterionic polymer to the nanorod surface. The TGA curve quantitatively determines the amount of the coupled polymer. After the loss of water molecules before 300°C, the polymer is decomposed until 580°C with a weight loss of 19.2%. The coverage density of the polymer on a single nanorod is then calculated to be 0.3 nm^{-2} (corresponding to 3 mg/m^2), which is close to the values reported on quantum dots.[27]

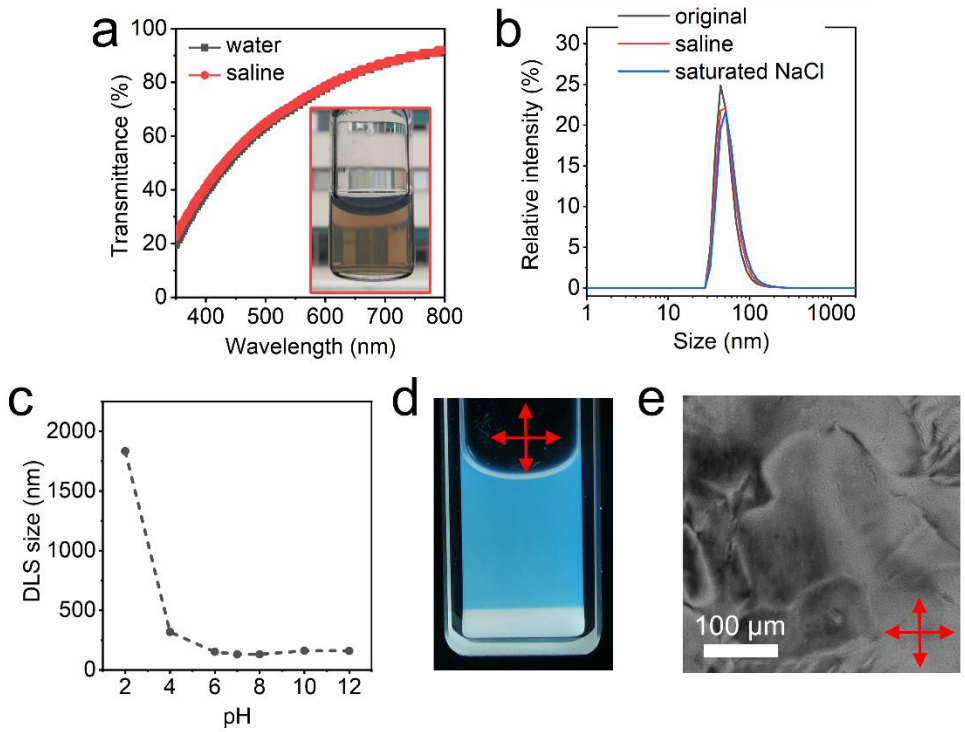

Figure 2. Colloidal stability of zwitterion functionalized $LaPO_4$:5%Eu^{3+} nanorods. (a) Transmittance spectra as a function of light wavelength for the suspensions in pure water and saline at the volume fraction Φ of 0.5% (25 g/L). The inset image shows the transparency of the saline suspension. (b) DLS measured hydrodynamic diameter of the bare nanorods in pH=2 water and the functionalized nanorods in saline and saturated NaCl solution. (c) DLS size as a function of pH value with fixed ionic strength of saline. (d) Macroscopic isotropic liquid-nematic phase separation of saline suspension (original Φ=6.5%, 325 g/L) in a 2 mm-think quartz cell with the corresponding birefringence for the bottom nematic phase under crossed polarizers. (e) A typical birefringent texture of the nematic sample observed by a polarizing microscope with crossed polarizers.

Colloidal Stability In physiological conditions, various ions from salts at elevated concentrations (e.g. Na^+ of 130-155 mM and K^+, Ca^{2+}, and Mg^{2+} of 1-5 mM)[43] and pH variation are always present and are generally detrimental to the colloidal stability of the suspension. To apply our nanorods in biofluids, it is necessary to verify the colloidal stability of the p(MAPC1-b-SBMA) functionalized nanorods under these conditions. After the zwitterion functionalization, the nanorods can be dispersed in various physiological media, such as saline (NaCl, 9 g/L) and DPBS (Dulbecco's phosphate buffered saline), typical physiological media used in biological study. The resulting saline suspension of the nanorods is transparent at a volume fraction of Φ=0.5% (25 g/L, approximatively 700 nM of nanorods), as shown in the inset of **Figure 2a**. Suspension transparency is close for pure water and saline. This is quantitatively confirmed by the transmittance spectra in **Figure 2a**, in which the transparency is 72% at 550 nm (close to 79% in the case of bare nanorods, **Figure S3**). The preserved high transparency indicates

that the present functionalization circumvents the particle aggregation at the physiological ionic strength of 0.15 M. Dynamic light scattering (DLS) measurements confirm the absence of aggregates with neglectable size increase (**Figure 2b**) and reveal the long-term colloidal stability for at least six months stored at room temperature (**Figure S4**). The colloidal stability was further examined under the extreme conditions of saturated NaCl solution (ionic strength of 6.0 M, **Figure 2b**) and highly concentrated $MgCl_2$ solution (ionic strength of 12 M, **Figure S5**). No aggregation occurs evidenced by the DLS results. This remarkable long-term tolerance for electrolytes is the uniqueness of zwitterions and has been observed when the SBMA function was involved.[31,44] This is explained by the enhanced solvation of zwitterionic polymer with high ionic strength as ions can screen the charges of the SBMA group to suppress the attractive interaction of the zwitterions.[45] Note that the DLS revealed size is always small than the actual size of the nanorods due to the anisotropic shape of particles.

Besides the high salt tolerance, pH tolerance was also examined in an extensive range (pH=2-12) by adding nitric acid or sodium hydroxide with the ionic strength of saline. In contrast to the instant precipitation when the pH value is increased beyond 3 for the bare nanorod suspension, the zwitterionic nanorod suspension retains colloidal stability over a wide pH range of 6 to 12 (**Figure 2c**). In the physiological pH conditions (pH=7.2), the surface zeta potential (**Figure S6**) is highly negative at -41±1 mV. Colloidal stability does not however rely on electrostatic repulsion between nanorods only, since they remain stable even under extremely high ionic strength, where electrostatic interactions are efficiently screened. Instead, it relies on steric stabilization due to the very hydrophilic zwitterionic polymers. Surface charge increases when the pH value deviates from the neutral pH, but still is negative. The negative charge has been observed for some zwitterionic functionalizations[45-47] although in principle the net charge is close to zero due to the compensated counter ions. In our case, the negative charge is intrinsic to the polymer structure. Phosphonic acids can be deprotonated under neutral pH conditions as the acid dissociation constants (pKa) of the phosphoric acid are 1.3 and 6.7 for the first and second dissociation.[48] Because of the second dissociation, the zeta potential steeply rises from -41±1 mV at pH=7 to -17±1 mV at pH=6. At pH 2 to 4, the nanorods tend to aggregate, which can be interpreted by the over protonated phosphonate group, resulting in the gradual decoupling of the p(MAPC1-b-SBMA) zwitterionic polymer from the nanorod surface. Note that the nanorods remain stable in the biologically relevant pH range, an important point for their biological applications.

Good colloidal stability has been validated at a moderate particle concentration (Φ=0.5%). To further examine the colloidal stability, the nanorod concentration was largely increased. In comparison, the same functionalization was conducted under sonication (**Figure S7**). At moderate concentrations of the nanorods, the suspension is transparent as in the case of microwave heating. Nevertheless, aggregation occurs at high concentrations. Instead of tending to aggregate, the concentrated nanorods under microwave heating (Φ=3.5%) dispersed in pure water (pH=7) exhibit liquid crystalline behaviors that were also observed on the bare nanorods under acidic conditions (pH=2).[40] The contrast experiments validate the importance of microwave heating towards the

successful functionalization of the zwitterionic polymers on the nanorod surface. Importantly, the occurrence of the liquid crystalline behaviors suggests the limited influence of the zwitterionic polymer on the self-alignment of the nanorods. This preserved orientability of zwitterionic nanorods paves the way for the application of the nanorods in biofluids. More interestingly, the liquid crystalline phenomenon remains in saline (Φ=6.5%), further confirming the extraordinary colloidal stability of the zwitterionic functionalization realized by microwave heating. **Figure 2d** shows the phase separation in saline: the upper isotropic part (randomly oriented nanorods) and the bottom nematic part (self-aligned nanorods). Under crossed polarizers, the nematic domain transmits light presenting strong birefringence. A typical image of birefringence is displayed in **Figure 2e** for the nematic sample taken on a polarizing optical microscope. To our knowledge, it is the first report on liquid crystalline behaviors on artificially synthesized nanocrystals in physiological media, although self-ordering of living macromolecule entities is common in nature, such as the lipid bilayer membrane assembled by hydrophobic interactions.[49]

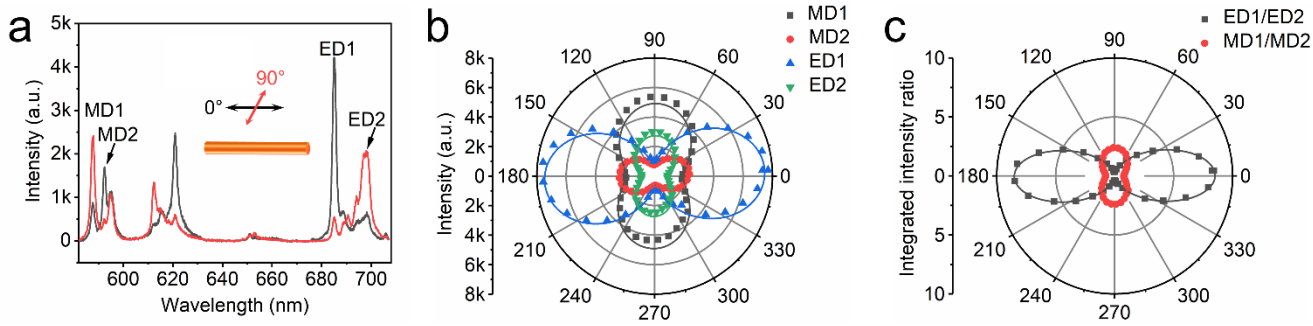

Figure 3. Polarized luminescence properties of zwitterionic $LaPO_4$:5%Eu^{3+} nanorods in a nematic phase. (a) Polarized emission spectra under 394 nm laser excitation with a schematic illustration of emission observation from nanorods by changing the polarizer from 0° to 90° (parallel and perpendicular to the nanorod orientation). The most polarized emission lines are labeled as MD1 and MD2 in the magnetic dipole transition of $^5D_0$-$^7F_1$ and ED1 and ED2 in the forced electric dipole transition of $^5D_0$-$^7F_4$. (b) Polar diagrams of the integrated intensity (MD1, MD2, ED1, and ED2) with fitting plots. (c) Ratiometric polar diagrams of the integrated intensity ratios (MD1/MD2 and ED1/ED2) with fitting plots.

Polarized Emission The superior colloidal stability of the physiological suspension with the zwitterionic functionalized nanorods paves the way to utilize the nanorods for the orientation analysis in biological systems. The nanorods in our study are aimed at monitoring the shear stress in dynamic biofluids. The methodology of the orientation analysis relies on the Eu^{3+} polarized emission.[13,50] The polarization measurements were performed by rotating a polarizer in the emission path. The emission intensity for each transition was detected to change with the polarizer angle (θ), the difference between the polarization axis and the nanorod orientation. Specifically, the polarizer angle of 0° or 90°

means that the polarizer is parallel or perpendicular to the nanorod orientation, resulting in a spectrum in π or σ configuration. **Figure 3a** shows the polarized emission spectra for the in-plane nematic sample (**Figure 2e**) under 394 nm laser excitation. The emission consists of defined lines split by the crystal field and is generated from the magnetic dipole (MD) transitions of $^5D_0$-$^7F_1$ (587 and 592 nm as MD1 and MD2) and the forced electric dipole (ED) transitions of $^5D_0$-$^7F_2$ (612 and 621 nm) and $^5D_0$-$^7F_4$ (685 and 698 nm as ED1 and ED2).[51] Each emission line varies periodically in intensity via rotating the polarizer. The dominant emission lines are strongly polarized. The polarized emission spectra in **Figure 3a** are similar to those taken from the nematic domain of the bare nanorod in ethylene glycol (**Figure S8**) under the same experimental conditions,[40] further confirming the neglectable effect of the coupling zwitterionic polymers on the self-alignment of the nanorods. When the nanorods in this study are used in probing biofluid dynamics, current polarized emission spectra will serve as a reference to determine the orientation of collective nanorods or a single nanorod. Note that although the p(MAPC1-b-SBMA) zwitterionic polymer can absorb and emit light (**Figure S1**), the bands are far away from the absorption and emission of Eu^{3+} ions. Hence, there is no energy transfer between the coupled p(MAPC1-b-SBMA) zwitterionic polymer and Eu^{3+} ions inside the nanorods, as evidenced by the identical emission spectra (**Figure S9**) before and after the functionalization. This demonstrates the unaltered sensitivity and accuracy of orientation analysis after the zwitterionic functionalization.

To do quantitative analysis on polarized emission, **Figure 3b** plots the polar diagrams for the integrated emission intensity of MD1, MD2, ED1, and ED2 transitions as a function of θ in every 10°. The data points are fitted with a simple trigonometric function: $I_\theta = I_\pi \cdot \cos^2\theta + I_\sigma \cdot \sin^2\theta$, where I_π and I_σ denote the integrated emission intensity with θ at 0° and 90°. The fits are good showing a dumbbell shape of the polar diagrams for each transition dipole. The fitting data is used to quantify the degree of polarization (DOP=$(I_\pi - I_\sigma)/(I_\pi + I_\sigma)$). DOP is calculated to be as high as -0.43, 0.55, 0.79, and -0.51 for the MD1, MD2, ED1, and ED2 emission lines. High DOPs are expected from the highly aligned nanorods in the nematic sample, providing high accuracy to the orientation analysis.[13,50] However, the deviation can be observed between the data points and the fits. This is due to a slight distortion of the emission beam upon rotating the polarizer and a slight intensity fluctuation of the laser excitation. To avoid global intensity fluctuation, integrated intensity ratios can be applied to enhance the accuracy of the orientation analysis.[50,52] The ratiometric polar diagrams in **Figure 3c** match perfectly with the fits for the MD1/MD2 and ED1/ED2 intensity ratios. The neck of the ED1/ED2 plot is extremely narrow, indicating a high DOP (0.93 and 0.52 for MD1/MD2).

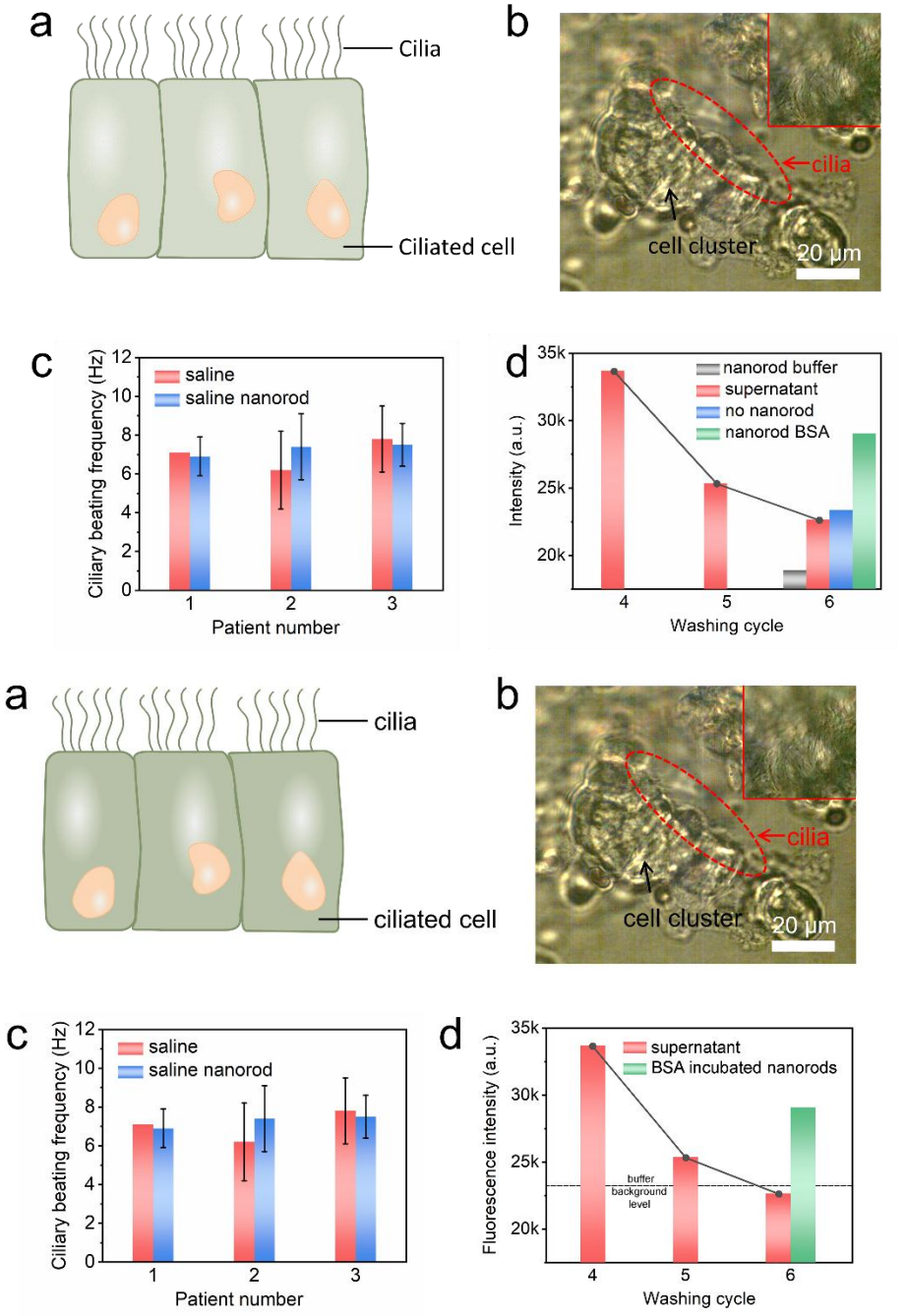

Figure 4. Biocompatibility of zwitterion functionalized $LaPO_4$:5%Eu^{3+} nanorods in the physiological media. (a) Schematic cartoon of the nasal respiratory ciliated cells and the cilia on one side. (b) A cluster of ciliary cells with the inset of cilia. (c) Beating frequency of ciliated cells in saline without and with nanorods (Φ=0.5%). (d) Fluorescence intensity of fluorescamine assay with different washing cycles (red column: supernatant after centrifugation for the nanorods incubated in buffer with BSA; green column: nanorods incubated in buffer with BSA after 6 washes; dashed line: buffer without nanorods and BSA).

Biocompatibility To mimic the real physiological conditions, the behaviors of the zwitterion-coupled nanorods were examined in more complex environments with living cells.[26,35,36,44] Here we choose the ciliated cells of the upper respiratory airway system of humans as the ciliated cells are sensitive to the surrounding environments and their functionality can be quantified by the ciliary beating frequency.[53] As shown in **Figure 4a, 4b** and **SI video**, cilia grow on the apical side of the cells. Ciliary beating generates flow in the surrounding medium with a strong steady component. Before applying the nanorod-based orientation analysis, it is of importance to know the mutual influence between the nanorods and the cells. Three batches of ciliated cells were mixed with the nanorod suspension separately. In saline (**Figure 4c**) and DPBS (**Figure S10**), the ciliary beating frequency is unchanged, indicating that the cilia functionality of the cells is not affected in the presence of the nanorod suspension. Given the extreme fragility of the cilia, these experiments evidence the non-toxicity of the nanorods and zwitterionic polymers.

In addition, the maintained beating frequency suggests null or limited binding of the zwitterionic nanorods on the cilia. In reality, the physiological environment is complex and rich in macromolecules, such as proteins and lipids. Nanocrystals can non-specifically interact with these components, which is undesired as it impairs both cellular dynamics and nanocrystal functionality.[21,54] To check the anti-fouling properties of the nanorods coated with the zwitterionic polymer, we investigated the amount of proteins strongly binding to the nanorods, corresponding to the "hard corona".[27] Adsorption of proteins on the nanorod surface was evaluated after incubation in bovine serum albumin (BSA), a commonly used model protein that is present at millimolar concentrations in the blood. The nanorods (0.027% volume fraction, 38 nM of nanorods) were incubated with BSA (1 mM, 26,000 BSA per nanorod) for 1 h and then isolated from free and loosely bound proteins by several centrifugation cycles. The tightly bound proteins forming the hard corona were quantified by a fluorescamine assay. After calibration with known BSA concentrations, this assay provides an average number of BSA proteins bound per NR. The detection threshold, obtained using the standard deviation of the blank measurement, is 0.16 BSA per nanorod. In **Figure 4d**, fluorescence measurements indicate that six washes can completely remove the unbound BSA proteins. The corresponding precipitation contains the nanorods with non-specific bound proteins. We found that a single nanorod can bind 0.8 BSA on average: there is 1 BSA per 6,000 nm^2 of nanorod surface, which is an extremely low level of non-specific interaction thanks to the zwitterions.[36,55]

CONCLUSIONS

In summary, monazite $LaPO_4$:5%Eu^{3+} nanorods have been successfully functionalized by zwitterionic block copolymers. Due to the high affinity of the phosphonate group to the nanorod and the zwitterionic nature, the corresponding nanorods are long-term stable in physiological media over a large range of pH values and in the presence of extremely high concentrations of salts. The liquid crystalline behaviors are also retained when the

nanorods are concentrated. In this case, the ability of shear alignment for the nanorods are unaltered in the presence of the coated polymers and thus the strongly polarized Eu^{3+} emission can be observed. The zwitterionic functionalization in this study also enables good biocompatibility of the nanorods, i.e. non-toxicity and limited non-specific interaction. Therefore, the zwitterionic nanorods can be applied to the orientation analysis in biofluids, but also in a broad range of bio-applications. Further modification of the zwitterions can enable the nanorods with access to bioconjugates as targeting probes. We believe that our study will arouse further research on the design and application of zwitterionic ligands incorporated with lanthanide-doped nanocrystals.

ASSOCIATED CONTENT

Supporting Information

The following files are available free of charge.
Experimental details, characterization methods, photoluminescence spectra, FT-IR, transmittance spectra, DLS, zeta potential, and beating frequency of ciliated cells (PDF)

AUTHOR INFORMATION

Corresponding Authors

Jongwook Kim: jong-wook.kim@polytechnique.edu
Thierry Gacoin: thierry.gacoin@polytechnique.edu

Conflicts of interest

There are no conflicts to declare.

ACKNOWLEDGMENT

This research was supported by the Fondation pour la Recherche Médicale (DCM20181039556, programme Chimie pour la Médecine), Institut Polytechnique de Paris (2020MATU0376), and the French national research agency (ANR-19-CE09-0033, ANR-10-EQPX-0050).

REFERENCES

1. Liu, Y.; Tu, D.; Zhu, H.; Chen, X. Lanthanide-doped luminescent nanoprobes: controlled synthesis, optical spectroscopy, and bioapplications. *Chem. Soc. Rev.* **2013**, *42*, 6924-6958.
2. Burrows, N. D.; Vartanian, A. M.; Abadeer, N. S.; Grzincic, E. M.; Jacob, L. M.; Lin, W.; Li, J.; Dennison, J. M.; Hinman, J. G.; Murphy, C. J. Anisotropic nanoparticles and anisotropic surface chemistry. *J. Phys. Chem. Lett.* **2016**, *7*, 632-641.

3. Wang, J.; Gudiksen, M. S.; Duan, X.; Cui, Y.; Lieber, C. M. Highly polarized photoluminescence and photodetection from single indium phosphide nanowires. *Science* **2001**, *293*, 1455-1457.
4. Yan, R.; Sun, X.; Wang, X.; Peng, Q.; Li, Y. Crystal structures, anisotropic growth, and optical properties: controlled synthesis of lanthanide orthophosphate one- dimensional nanomaterials. *Chem. - Eur. J.* **2005**, *11*, 2183-2195.
5. Shi, S.; Sun, L.; Xue, Y.; Dong, H.; Wu, K.; Guo, S.; Wu, B.; Yan, C. Scalable direct writing of lanthanide-doped $KMnF_3$ perovskite nanowires into aligned arrays with polarized up-conversion emission. *Nano Lett.* **2018**, *18*, 2964-2969.
6. Yang, D.; Peng, Z.; Guo, X.; Qiao, S.; Zhao, P.; Zhan, Q.; Qiu, J.; Yang, Z.; Dong, G. Tunable light polarization information from single upconverting fluoride microcrystal. *Adv. Opt. Mater.* **2021**, *9*, 2100044.
7. Mundoor, H.; Smalyukh, I. I. Mesostructured composite materials with electrically tunable upconverting properties. *Small* **2015**, *11*, 5572-5580.
8. Ohmachi, M.; Komori, Y.; Iwane, A. H.; Fujii, F.; Jin, T.; Yanagida, T. Fluorescence microscopy for simultaneous observation of 3D orientation and movement and its application to quantum rod-tagged myosin V. *Proc. Natl. Acad. Sci.* **2012**, *109*, 5294-5298.
9. Rodríguez-Sevilla, P.; Zhang, Y.; de Sousa, N.; Marqués, M. I.; Sanz-Rodríguez, F.; Jaque, D.; Liu, X.; Haro-González, P. Optical torques on upconverting particles for intracellular microrheometry. *Nano Lett.* **2016**, *16*, 8005-8014.
10. Mundoor, H.; Wu, J.-S.; Wensink, H. H.; Smalyukh, I. I. Thermally reconfigurable monoclinic nematic colloidal fluids. *Nature* **2021**, *590*, 268-274.
11. Kim, J.; de la Cotte, A.; Deloncle, R.; Archambeau, S.; Biver, C.; Cano, J. P.; Lahlil, K.; Boilot, J. P.; Grelet, E.; Gacoin, T. $LaPO_4$ mineral liquid crystalline suspensions with outstanding colloidal stability for electro‐optical applications. *Adv. Funct. Mater.* **2012**, *22* 4949-4956.
12. Shroder, D. Y.; Lippert, L. G.; Goldman, Y. E. Single molecule optical measurements of orientation and rotations of biological macromolecules. *Methods Appl. Fluoresc.* **2016**, *4*, 042004.
13. Kim, J.; Michelin, S.; Hilbers, M.; Martinelli, L.; Chaudan, E.; Amselem, G.; Fradet, E.; Boilot, J.-P.; Brouwer, A. M.; Baroud, C. N., Peretti, J.; Gacoin, T. Monitoring the orientation of rare-earth-doped nanorods for flow shear tomography. *Nat. Nanotech.* **2017**, *12*, 914-919.
14. Chen, G.; Qiu, H.; Prasad, P. N.; Chen, X. Upconversion nanoparticles: design, nanochemistry, and applications in theranostics. *Chem. Rev.* **2014**, *114*, 5161-5214.
15. Abdukayum, A.; Chen, J.; Zhao, Q.; Yan, X. Functional near infrared-emitting Cr^{3+}/Pr^{3+} co-doped zinc gallogermanate persistent luminescent nanoparticles with superlong afterglow for in vivo targeted bioimaging. *J. Am. Chem. Soc.* **2013**, *135*, 14125-14133.
16. Yao, C.; Wang, P.; Zhou, L.; Wang, R.; Li, X.; Zhao, D.; Zhang, F. Highly biocompatible zwitterionic phospholipids coated upconversion nanoparticles for efficient bioimaging. *Anal. Chem.* **2014**, *86*, 9749-9757.
17. Guo, T.; Lin, Y.; Zhang, W.; Hong, J.; Lin, R.; Wu, X.; Li, J.; Lu, C.; Yang, H. High-efficiency X-ray luminescence in Eu^{3+}-activated tungstate nanoprobes for optical imaging through energy transfer sensitization. *Nanoscale* **2018**, *10*, 1607-1612.

18. Di, X.; Wang, D.; Zhou, J.; Zhang, L.; Stenzel, M. H.; Su, Q. P.; Jin, D. Quantitatively monitoring in situ mitochondrial thermal dynamics by upconversion nanoparticles. *Nano Lett.* **2021**, *21*, 1651-1658.
19. Choi, H. S.; Liu, W.; Misra, P.; Tanaka, E.; Zimmer, J. P.; Ipe, B. I.; Bawendi, M. G.; Frangioni, J. V. Renal clearance of quantum dots. *Nat. Biotechnol.* **2007**, *25*, 1165-1170.
20. Estephan, Z. G.; Schlenoff, P. S.; Schlenoff, J. B. Zwitteration as an alternative to PEGylation. *Langmuir* **2011**, *27*, 6794-6800.
21. García, K. P.; Zarschler, K.; Barbaro, L.; Barreto, J. A.; O'Malley, W.; Spiccia, L.; Stephan, H.; Graham, B. Zwitterionic- coated "stealth" nanoparticles for biomedical applications: recent advances in countering biomolecular corona formation and uptake by the mononuclear phagocyte system. *Small* **2014**, *10*, 2516-2529.
22. Ostuni, E.; Chapman, R. G.; Holmlin, R. E.; Takayama, S.; Whitesides, G. M. A survey of structure-property relationships of surfaces that resist the adsorption of protein. *Langmuir* **2001**, *17*, 5605-5620.
23. Chen, S.; Zheng, J.; Li, L.; Jiang, S. Strong resistance of phosphorylcholine self-assembled monolayers to protein adsorption: insights into nonfouling properties of zwitterionic materials. *J. Am. Chem. Soc.* **2005**, *127*, 14473-14478.
24. Shao, Q.; Jiang, S. Molecular understanding and design of zwitterionic materials. *Adv. Mater.* **2015**, *27*, 15-26.
25. Jiang, S.; Cao, Z. Ultralow- fouling, functionalizable, and hydrolyzable zwitterionic materials and their derivatives for biological applications. *Adv. Mater.* **2010**, *22*, 920-932.
26. Wang, W.; Ji, X.; Kapur, A.; Zhang, C.; Mattoussi, H. A multifunctional polymer combining the imidazole and zwitterion motifs as a biocompatible compact coating for quantum dots. *J. Am. Chem. Soc.* **2015**, *137*, 14158-14172.
27. Debayle, M.; Balloul, E.; Dembele, F.; Xu, X.; Hanafi, M.; Ribot, F.; Monzel, C.; Coppey, M.; Fragola, A.; Dahan, M.; Pons, T.; Lequeux, N. Zwitterionic polymer ligands: an ideal surface coating to totally suppress protein-nanoparticle corona formation? *Biomaterials* **2019**, *219*, 119357.
28. Shao, Q.; He, Y.; White, A. D.; Jiang, S. Difference in hydration between carboxybetaine and sulfobetaine. *J. Phys. Chem. B* **2010**, *114*, 16625-16631.
29. Wei, H.; Insin, N.; Lee, J.; Han, H.-S.; Cordero, J. M.; Liu, W.; Bawendi, M. G. Compact zwitterion-coated iron oxide nanoparticles for biological applications. *Nano Lett.* **2012**, *12*, 22-25.
30. Kievit, F. M.; Zhang, M. Cancer nanotheranostics: improving imaging and therapy by targeted delivery across biological barriers. *Adv. Mater.* **2011**, *23*, H217-H247.
31. Giovanelli, E.; Muro, E.; Sitbon, G.; Hanafi, M.; Pons, T.; Dubertret, B.; Lequeux, N. Highly enhanced affinity of multidentate versus bidentate zwitterionic ligands for long-term quantum dot bioimaging. *Langmuir* **2012**, *28*, 15177-15184.
32. Zhan, N.; Palui, G.; Safi, M.; Ji, X.; Mattoussi, H. Multidentate zwitterionic ligands provide compact and highly biocompatible quantum dots. *J. Am. Chem. Soc.* **2013**, *135*, 13786-13795.
33. Yao, C.; Wei, C.; Huang, Z.; Lu, Y.; El-Toni, A. M.; Ju, D.; Zhang, X.; Wang, W.; Zhang, F. Phosphorylated peptide functionalization of lanthanide upconversion

nanoparticles for tuning nanomaterial–cell interactions. *ACS Appl. Mater. Interfaces* **2016**, *8*, 6935-6943.
34. Delille, F.; Pons, T.; Lequeux, N. Poly(sulfobetaine-phosphonate) block copolymers as ultrastable and antifouling iron oxide nanoparticle surface chemistry. In preparation.
35. Tasso, M.; Giovanelli, E.; Zala, D.; Bouccara, S.; Fragola, A.; Hanafi, M.; Lenkei, Z.; Pons, T.; Lequeux, N. Sulfobetaine–vinylimidazole block copolymers: a robust quantum dot surface chemistry expanding bioimaging's horizons. *ACS Nano* **2015**, *9*, 11479-11489.
36. Trapiella-Alfonso, L.; Pons, T.; Lequeux, N.; Leleu, L.; Grimaldi, J.; Tasso, M.; Oujagir, E.; Seguin, J.; D'orlyé, F.; Girard, C. Clickable-zwitterionic copolymer capped-quantum dots for in vivo fluorescence tumor imaging. *ACS Appl. Mater. Interfaces* **2018**, *10*, 17107-17116.
37. Yao, C.; Wang, P.; Wang, R.; Zhou, L.; El-Toni, A. M.; Lu, Y.; Li, X.; Zhang, F. Facile peptides functionalization of lanthanide-based nanocrystals through phosphorylation tethering for efficient in vivo NIR-to-NIR bioimaging. *Anal. Chem.* **2016**, *88*, 1930-1936.
38. Duong, H. T.; Chen, Y.; Tawfik, S. A.; Wen, S.; Parviz, M.; Shimoni, O.; Jin, D. Systematic investigation of functional ligands for colloidal stable upconversion nanoparticles. *RSC Adv.* **2018**, *8*, 4842-4849.
39. Jesson, C. P.; Pearce, C. M.; Simon, H.; Werner, A.; Cunningham, V. J.; Lovett, J. R.; Smallridge, M. J.; Warren, N. J.; Armes, S. P. H_2O_2 enables convenient removal of RAFT end-groups from block copolymer nano-objects prepared via polymerization-induced self-assembly in water. *Macromolecules* **2017**, *50*, 182-191.
40. Wang, Z.; Kim, J.; Magermans, L.; Corbella, F.; Florea, I.; Larquet, E.; Kim, J.; Gacoin, T. Monazite $LaPO_4$:Eu^{3+} nanorods as strongly polarized nano-emitters. *Nanoscale* **2021**, *13*, 16968-16976.
41. de Sousa Filho, P. C.; Serra, O. A. Reverse microemulsion synthesis, structure, and luminescence of nanosized $REPO_4$: Ln^{3+} (RE= La, Y, Gd, or Yb, and Ln= Eu, Tm, or Er). *J. Phys. Chem. C* **2011**, *115*, 636-646.
42. Solimando, X.; Kennedy, E.; David, G.; Champagne, P.; Cunningham, M. F. Phosphorus-containing polymers synthesised via nitroxide-mediated polymerisation and their grafting on chitosan by grafting to and grafting from approaches. *Polym. Chem.* **2020**, *11*, 4133-4142.
43. Maughan, R. J.; Watson, P.; Shirreffs, S. M. Implications of active lifestyles and environmental factors for water needs and consequences of failure to meet those needs. *Nutr. Rev.* **2015**, *73*, 130-140.
44. Muro, E.; Pons, T.; Lequeux, N.; Fragola, A.; Sanson, N.; Lenkei, Z.; Dubertret, B. Small and stable sulfobetaine zwitterionic quantum dots for functional live-cell imaging. *J. Am. Chem. Soc.* **2010**, *132*, 4556-4557.
45. Mary, P.; Bendejacq, D. D.; Labeau, M.-P.; Dupuis, P. Reconciling low-and high-salt solution behavior of sulfobetaine polyzwitterions. *J. Phys. Chem. B* **2007**, *111*, 7767-7777.
46. Polzer, F.; Heigl, J.; Schneider, C.; Ballauff, M.; Borisov, O. V. Synthesis and analysis of zwitterionic spherical polyelectrolyte brushes in aqueous solution. *Macromolecules* **2011**, *44*, 1654-1660.

47. Dong, Z.; Mao, J.; Yang, M.; Wang, D.; Bo, S.; Ji, X. Phase behavior of poly (sulfobetaine methacrylate)-grafted silica nanoparticles and their stability in protein solutions. *Langmuir* **2011**, *27*, 15282-15291.
48. Haynes, W. M., Lide, D. R., Bruno, T. J. CRC handbook of chemistry and physics, 97th ed.; CRC Press, **2016**.
49. Mouritsen, O. G.; Bagatolli, L. A. Life-as a matter of fat, 1st ed.; Springer, **2005**.
50. Kim, J.; Chacón, R.; Wang, Z.; Larquet, E.; Lahlil, K.; Leray, A.; Colas-des-Francs, G.; Kim, J.; Gacoin, T. Measuring 3D orientation of nanocrystals via polarized luminescence of rare-earth dopants. *Nat. Commun.* **2021**, *12*, 1943.
51. Chaudan, E.; Kim, J.; Tusseau-Nenez, S.; Goldner, P.; Malta, O. L.; Peretti, J.; Gacoin, T. Polarized luminescence of anisotropic $LaPO_4$:Eu nanocrystal polymorphs. *J. Am. Chem. Soc.* **2018**, *140*, 9512-9517.
52. Brites, C. D.; Lima, P. P.; Silva, N. J.; Millán, A.; Amaral, V. S.; Palacio, F.; Carlos, L. D. Thermometry at the nanoscale. *Nanoscale* **2012**, *4*, 4799-4829.
53. Bottier, M.; Blanchon, S.; Pelle, G.; Bequignon, E.; Isabey, D.; Coste, A.; Escudier, E.; Grotberg, J. B.; Papon, J.-F.; Filoche, M. A new index for characterizing micro-bead motion in a flow induced by ciliary beating: part I, experimental analysis. *PLoS Comput. Biol.* **2017**, *13*, e1005605.
54. Park, J.; Nam, J.; Won, N.; Jin, H.; Jung, S.; Jung, S.; Cho, S. H.; Kim, S. Compact and stable quantum dots with positive, negative, or zwitterionic surface: specific cell interactions and non- specific adsorptions by the surface charges. *Adv. Funct. Mater.* **2011**, *21*, 1558-1566.
55. Muro, E.; Fragola, A.; Pons, T.; Lequeux, N.; Ioannou, A.; Skourides, P.; Dubertret, B. Comparing intracellular stability and targeting of sulfobetaine quantum dots with other surface chemistries in live cells. *Small* **2012**, *8*, 1029-1037.

TOC

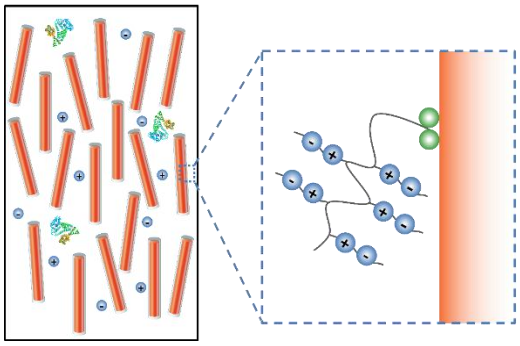

We report an efficient surface functionalization of zwitterionic polymer on strongly polarized nano-emitters. Outstanding colloidal stability and biocompatibility enable their use as bioprobes.